

Analysis of Structural Shock Transmission

Peter Crimi*

Avco Systems Division, Wilmington, Mass.

An analytic procedure is developed for evaluating response of a shock-loaded structure at some point, given only the response at some other point. A specific system is analyzed and the results compared with test data. Capability of the procedure to predict transmitted shock response is first demonstrated. An acceleration time history is then synthesized from a shock spectrum, as a sum of damped sinusoids, and used to predict shock response. Lastly, the response in the vicinity of the point of shock loading is predicted by numerical integration using a simplified model of the structure. The response so obtained is then used as input to predict transmitted shock response, demonstrating that response throughout a shock-loaded structure can be predicted without resorting to numerical simulation using a complete model.

I. Introduction

STRUCTURAL design frequently requires definition of the dynamic environment resulting from shock loading. For example, limitations imposed on the shock-induced acceleration to which spacecraft instrumentation can be subjected in turn dictate design requirements for related structural elements to achieve acceptable isolation from boost and separation shock events.

In theory, prediction of structural response to shock loading should be straightforward, assuming the system to be analyzed is adequately modeled with a finite number of degrees of freedom using, say, a lumped-mass or finite-element formulation,¹ and the physics of the shock is well defined. There are several methods currently in use for integrating coupled sets of ordinary differential equations that are applicable to shock-response analysis.^{2,3} However, in certain instances, a great many degrees of freedom are required to represent the system, either because the complexity of the structure precludes a more manageable formulation or because it is necessary to accurately define the high-frequency response at some point in the structure. Accurate integration of the equations of motion can then become extremely arduous and costly,⁴ while at the same time producing large quantities of information not needed for the problem at hand, since the response at only certain locations in the structure are of interest.

A procedure has been developed, as described in what follows, for evaluating the transient response at a specified point of a structure given only the response at some other point. Three different applications of the procedure in shock-response analysis have been identified. First, if response to shock loading is measured at some point during flight or ground tests, the response at other points that were not instrumented can be calculated by this procedure.

With regard to the second application, the designer is sometimes confronted with a specification for shock severity at some location, e.g., the booster/payload interface, which is given in the form of a shock spectrum[†] of the response there,

while the shock response at some other location is needed. A procedure has been developed for synthesizing an acceleration time history from a shock spectrum. This acceleration can then be employed to evaluate the response at other locations in the structure, using the procedures developed. While the acceleration input so derived is, of course, not unique, as it would be if Fourier spectra were used in shock specifications, the predicted responses at other points in the structure have been found to agree quite well with measurements when the input was synthesized from a spectrum derived from measured response.

With regard to the third application, in many instances the response in the immediate vicinity of the point of application of a shock loading can be accurately simulated with a model having only a few degrees of freedom. With the response obtained in this way, transmission of the shock to more distant points can be evaluated, by the procedure developed, without the need for a simulation using a complete model.

In what follows, the basic formulations employed to evaluate shock transmission are first developed and a method for synthesizing an acceleration time history from a shock spectrum is outlined. Examples of the three applications described above are then given.

II. Formulations

Response at a Specified Point

Consider a structure subjected to shock loading that is represented by a linear system with N degrees of freedom. The equations of motion of the system are of the form

$$M\ddot{X} + C\dot{X} + KX = F \quad (1)$$

where M , C , and K are mass, damping and stiffness matrices, respectively, whereas X and F are displacement and force vectors, respectively. It is assumed, first, that only one inertial element, say the first, is subjected to shock loading,[‡] initiated at time $t=0$, so that the first element of F is some function $f(t)$, whereas all other elements of F are zero. It is also assumed that all displacements and rates are initially zero.

Taking the Laplace transform of Eq. (1), then, it follows that

$$[s^2M + sC + K]\bar{X} = \bar{F} \quad (2)$$

where s is the independent variable of the transformed equations, whereas \bar{X} and \bar{F} are vectors, the elements of which

Received Sept. 19, 1977; revision received Dec. 19, 1977. Copyright © American Institute of Aeronautics and Astronautics, Inc., 1978. All rights reserved.

Index categories: Structural Dynamics; Analytical and Numerical Methods; LV/M Structural Design (including Loads).

*Senior Consulting Engineer. Member AIAA.

†The characterization of an acceleration time history known as a shock spectrum has been variously defined.⁵ A shock spectrum is defined here to be the envelope of the magnitude of the maximum acceleration, relative to an inertial frame, of an ensemble of linear oscillators having 5% of critical damping, the bases of which are subjected to the given acceleration time history.

‡The procedure developed can in fact be generalized, if necessary, to account for shock loading imposed on two or more inertial elements simultaneously.

are the Laplace transforms of the displacement and force vector elements.

Using Cramer's rule to solve Eq. (2) for the elements \bar{x}_m ($m=1,2,\dots,N$) of \bar{X} , it is found that

$$\bar{x}_m = \bar{f}(s) \Delta_m(s) / \Delta_0(s) \quad (3)$$

where $\bar{f}(s)$ is the Laplace transform of $f(t)$, Δ_0 is the determinant of $[s^2 M + sC + K]$, and Δ_m is an $(N-1) \times (N-1)$ determinant. If $a_{mn} = m_{mn}s^2 + c_{mn}s + k_{mn}$, where m_{mn} , c_{mn} , and k_{mn} are the m th elements of M , C , and K , respectively, then

$$\Delta_m(s) = (-1)^{m+1} \begin{vmatrix} a_{21} & a_{22} & \dots & a_{2,m-1} & a_{2,m+1} & \dots & a_{2N} \\ a_{32} & a_{33} & \dots & a_{3,m-1} & a_{3,m+1} & \dots & a_{3N} \\ \vdots & \vdots & \ddots & \vdots & \vdots & \ddots & \vdots \\ a_{N1} & a_{N2} & \dots & a_{N,m-1} & a_{N,m+1} & \dots & a_{NN} \end{vmatrix}$$

Now it is assumed that the response of inertial element r , $x_r(t)$, is known, and that the variation of x_m is desired. It follows from Eq. (3) that

$$\bar{x}_m(s) = \bar{g}_{mr}(s) \bar{x}_r(s) \quad (4)$$

where

$$\bar{g}_{mr}(s) = \Delta_m(s) / \Delta_r(s) \quad (5)$$

Applying the convolution theorem for Laplace transforms to Eq. (4), it follows that

$$x_m(t) = \int_0^t g_{mr}(t-\tau) x_r(\tau) d\tau \quad (6)$$

where g_{mr} is the inverse Laplace transform of \bar{g}_{mr} . It should be noted here that Eq. (6) is still valid if x_m and x_r are both replaced by their second derivatives, since initial displacements and rates are zero.

Evaluation of the Function g_{mr}

It is seen by expanding out the determinants in Eq. (5) that \bar{g}_{mr} is the ratio of two polynomials in s , each of which is, in general, of degree $2(N-1)$. The coefficients in the polynomials are sums of products of the m 's, c 's, and k 's. Clearly it would not be practical for any but the simplest of systems to develop the inverse Laplace transform of \bar{g}_{mr} in general analytic form.

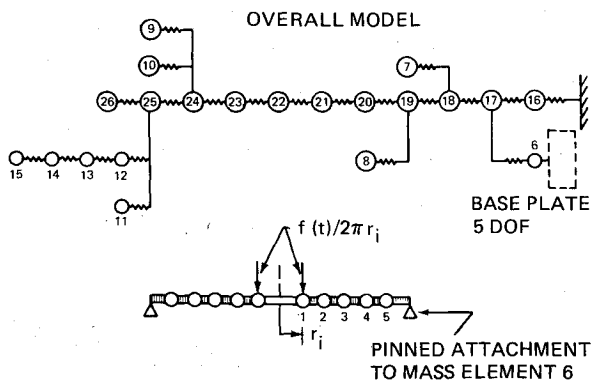


Fig. 1 Model of system analyzed.

However, Eq. (5) can be rewritten in the following form:

$$\bar{g}_{mr}(s) = A_0 + \sum_{n=1}^{N-1} \frac{A_n + B_n s}{s^2 + 2\zeta_n \omega_n s + \omega_n^2} \quad (7)$$

where the A_n 's, B_n 's, ω_n 's, and ζ_n 's are constants. The roots of the quadratics in s in Eq. (7) are zeros of $\Delta_r(s)$. Those zeros can be obtained by standard methods, for a given system, from which the values of the ω_n 's and ζ_n 's can be calculated directly. Thus, if the values of the A_n 's and B_n 's are known, $g_{mr}(t)$ is completely defined, since the inverse Laplace transform of Eq. (7) is readily obtained. For example, if all roots of Δ_r are complex conjugate pairs and all ζ_n 's are less than one, which is the case for the specific system analyzed in the next section, it is found that

$$g_{mr}(t) = A_0 \delta(t) + \sum_{n=1}^{N-1} e^{-\zeta_n \omega_n t} \times \left[\left(\frac{A_n}{\omega_n} - \frac{\zeta_n}{\sqrt{1-\zeta_n^2}} B_n \right) \sin \omega_n t + B_n \cos \omega_n t \right]$$

where $\tilde{\omega}_n = \omega_n \sqrt{1-\zeta_n^2}$, and $\delta(t)$ is the Dirac delta function.

It remains, then, to determine the A_n 's and B_n 's. This can be done by successively substituting $N-1$ values of s in Eq. (7) and calculating the required values of $\bar{g}_{mr}(s)$ from Eq. (5) to yield $N-1$ complex algebraic equations or $2(N-1)$ real linear algebraic equations for the A_n 's and B_n 's. If all ζ_n 's are small but nonzero, a well conditioned set of equations is obtained by choosing $s = i\omega_k$ ($k=1,2,\dots,N-1$), as the points at which \bar{g}_{mr} is evaluated. Specifically, in this instance, the A_n 's and B_n 's can be obtained from the following set of equations:

$$A_0 = \lim_{\omega \rightarrow \infty} \frac{\Delta_m(i\omega)}{\Delta_r(i\omega)}$$

$$\sum_{n=1}^{N-1} \frac{A_n + i\omega_k B_n}{\omega_n^2 - \omega_k^2 + 2i\zeta_n \omega_n \omega_k} = \frac{\Delta_m(i\omega_k)}{\Delta_r(i\omega_k)} - A_0$$

$$(k=1,2,\dots,N-1) \quad (9)$$

For a given system, then, the values of the A_n 's and B_n 's are obtained from the solution of Eq. (9) and substituted into Eq. (8). Evaluation of the integral in Eq. (6) then provides the response of the m th mass, given $x_r(t)$.

Synthesis of Acceleration Input from a Shock Spectrum

In some circumstances, a design requirement is imposed by specification of a shock spectrum of the response at a certain location, whereas the dynamic response at some other location in the structure must be evaluated. The following procedure can be employed to synthesize an acceleration time history that in turn can be substituted into Eq. (6) to evaluate the response elsewhere in the structure.

Let $S(f)$ denote the prescribed shock spectrum of the acceleration \ddot{x}_r , where S is maximum acceleration, in g 's, say, and f is frequency in Hz. It will be required that the shock spectrum of the synthesized \ddot{x}_r match S at N_s points with frequencies f_1, f_2, \dots, f_{N_s} .

The synthesized acceleration time history is taken to be of the form

$$\ddot{x}_r = \sum_{k=1}^{N_s} (-1)^k C_k e^{-\omega_k \zeta t} \sin(\omega_k t \sqrt{1-\zeta^2}) \quad (10)$$

where $\omega_k = 2\pi f_k$, the C_k 's are constants, and ζ is a free parameter. Computational effort can be excessive if ζ is very small; a value of 0.1 was found to give reasonable results economically.

The form specified by Eq. (10) was selected because shock response of actual structures (termed complex response in Ref. 5) typically resemble a sum of damped sinusoids. The alternating sign is simply for computational convenience.

The values of the coefficients in Eq. (10) are obtained iteratively, as follows. Let $S_c(C_1, C_2, \dots, C_{Ns}; f)$ denote the shock spectrum of \ddot{x}_r as calculated from Eq. (10). An initial estimate for the C_k 's is obtained by calculating S_c with one coefficient unity and all others zero; i.e.,

$$C_1^{(1)} = \frac{S(f_1)}{S_c(1, 0, 0, \dots, 0; f_1)} \quad C_2^{(1)} = \frac{S(f_2)}{S_c(0, 1, 0, \dots, 0; f_2)} \quad \text{etc.}$$

An iterative procedure is then carried out, using pseudopartial derivatives of S_c to correct the C_k 's. A weighting factor is used to avoid numerical instability. The iteration formula is

$$C_k^{(n+1)} = C_k^{(n)} + f_w \left[\frac{S(f_k) - S_c^{(n)}(f_k)}{\hat{S}_c(f_k) - S_c^{(n)}(f_k)} \right] \Delta C_k$$

where

$$S_c^{(n)}(f_k) = S_c(C_1^{(n)}, C_2^{(n)}, \dots, C_{Ns}^{(n)}; f_k)$$

$$\hat{S}_c(f_k) = S_c(C_1^{(n)}, C_2^{(n)}, \dots, C_k^{(n)} + \Delta C_k, \dots, C_{Ns}^{(n)}; f_k)$$

while ΔC_k is a specified fraction of $C_k^{(n)}$ (0.05 gives satisfactory results) and f_w is the weighting factor. Acceptable convergence is obtained with f_w equal to 0.5.

III. Analysis of a Specific System

System Analyzed

Shock transmission was analyzed for a structure consisting of an axially loaded conical shell with a 7.5 deg half-angle grounded at its base, closed near the base by a circular plate with a small circular hole in the middle, and containing several elastically mounted masses. The shell is modeled by concentrated masses connected by simple springs. The shock load is applied at the center of the base plate, which was modeled as an elastically continuous plate with the inertial load from five radially concentrated masses causing axisymmetric bending. The model, shown schematically in Fig. 1, has a

total of 26 degrees of freedom, the shock load being applied to concentrated mass numbered one. The natural frequencies for no damping and the corresponding normal modes were calculated and a damping matrix was constructed to give modal damping at 5% of critical. The undamped natural frequencies range from 154 to 32,720 Hz.

Shock tests of the actual structure were conducted and the response was measured with an accelerometer mounted immediately adjacent to mass no. 1. The response of mass no. 8 was of primary interest for purposes of component design. The response at that location was also measured, which provided data for comparison with predicted response.

The complex roots of Δ_l were calculated and the coefficients A_n and B_n in the function g_{sl} were evaluated using the previously described procedures. Results are listed in Table 1 (A_0 is zero).

To assess the accuracy with which the coefficients were obtained, the variation of $\hat{g}_{sl}(i\omega)$ was calculated from Eq. (5) for $\omega/2\pi$ from 0 to 34,000 Hz (the low-frequency portion of the result is shown in Fig. 2) and compared with the variation obtained using Eq. (7). Both real and imaginary parts agree to at least four places over the whole frequency range, so it appears that implementation of the formulations developed generally should not cause problems with numerical accuracy. It should be noted, however, that although values of the parameters in g_{sl} are listed in Table 1 to only three places, eight places were required in the computations to achieve this level of accuracy.

Response from Measured Input

The shock was imposed on the actual structure by suddenly releasing a large static load applied at the location of mass element no. 1. The acceleration time history measured there is shown in Fig. 3. This time history was used to calculate the response at mass no. 8, as prescribed by Eq. (6) (with displacements replaced by accelerations). The predicted variation of \ddot{x}_8 is shown in Fig. 4 together with the measured response at the location of mass no. 8 (note that the ordinate scales are not the same). The corresponding shock spectra are plotted in Fig. 5. The time histories are seen to agree quite well qualitatively (the sign convention for the measured acceleration is opposite that of the model). However, the predicted high-frequency peaks are somewhat larger than the

Table 1 Parameters of g_{sl}

n	A_n, s^{-2}	B_n, s^{-1}	$f_n/2\pi, \text{Hz}$	ζ_n
1	7.28×10^3	0.192	154	0.0499
2	3.57×10^4	0.835	201	0.0499
3	9.45×10^5	1.93	309	0.0499
4	-6.55×10^6	-12.1	771	0.0487
5	5.35×10^6	9.59	922	0.0426
6	2.91×10^4	0.0860	1150	0.0499
7	-2.05×10^4	-0.115	1320	0.0499
8	-3.00×10^4	-0.164	1990	0.0500
9	-1.48×10^3	-7.94×10^{-3}	2190	0.0500
10	3.68×10^3	0.0228	2820	0.0500
11	-6.15	-2.03×10^{-5}	2930	0.0500
12	139	-0.133	3480	0.0396
13	-7.85	-1.47×10^{-4}	3640	0.0500
14	2.44×10^3	-3.20×10^{-3}	3870	0.0500
15	4.66×10^3	-3.95×10^{-3}	4310	0.0500
16	-5.78×10^3	-5.67×10^{-3}	4360	0.0500
17	-5.73	-8.03×10^{-5}	5570	0.0500
18	-7.87	-3.27×10^{-5}	7390	0.0500
19	-102	-0.0266	10,100	0.0464
20	-13.6	-5.67×10^{-6}	11,700	0.0500
21	-16.4	-2.67×10^{-5}	13,600	0.0500
22	-13.3	-1.29×10^{-4}	15,100	0.0500
23	-55.2	-6.10×10^{-3}	20,200	0.0489
24	-31.1	-2.18×10^{-5}	28,700	0.0500
25	-31.9	-9.01×10^{-4}	32,500	0.0498

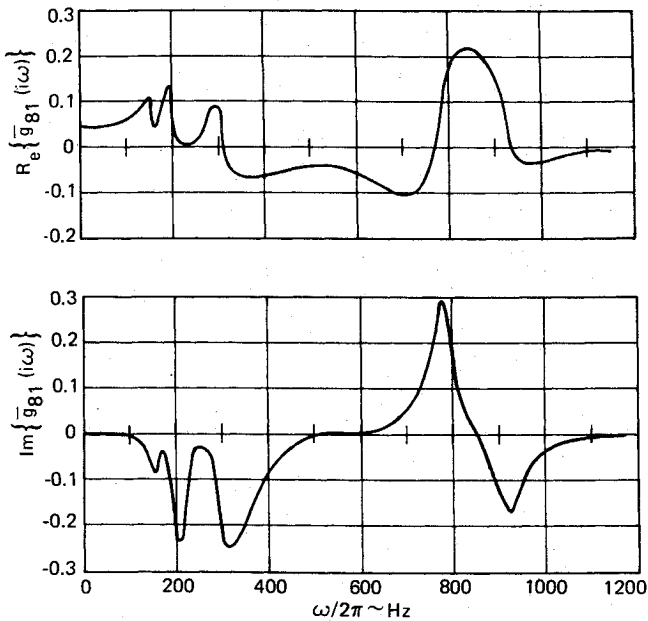


Fig. 2 Variation of \bar{g}_{8I} on the imaginary axis.

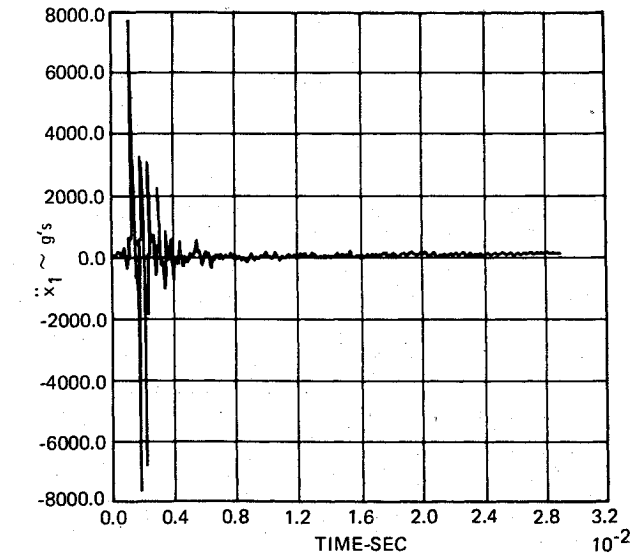


Fig. 3 Measured time history of \ddot{x}_I

measured ones. Similarly, the shock spectra are in good agreement at low frequency, but the theory is conservative in the vicinity of 1000 Hz. The differences can be attributed to insufficiencies in the modeling. Results of a brief sensitivity study indicate that a more refined representation of the conical shell is required. It can be concluded, however, that the formulations employed to predict the transmission of shock response function as intended.

Response from Synthesized Input

The procedure developed for synthesizing an acceleration time history was evaluated by constructing a time history, the spectrum of which approximates that of the measured \ddot{x}_I . The spectrum was fit at seven points, which are listed in Table 2, together with the calculated values of the C_k 's. Seven iterations were required. The synthesized time history is shown in Fig. 6 and its complete shock spectrum is plotted in Fig. 7 together with that of the measured acceleration. A seven-term series is seen to provide a very good fit.

The time history of \ddot{x}_8 was predicted from Eq. (6) using the synthesized \ddot{x}_I . The result is shown in Fig. 8, and the

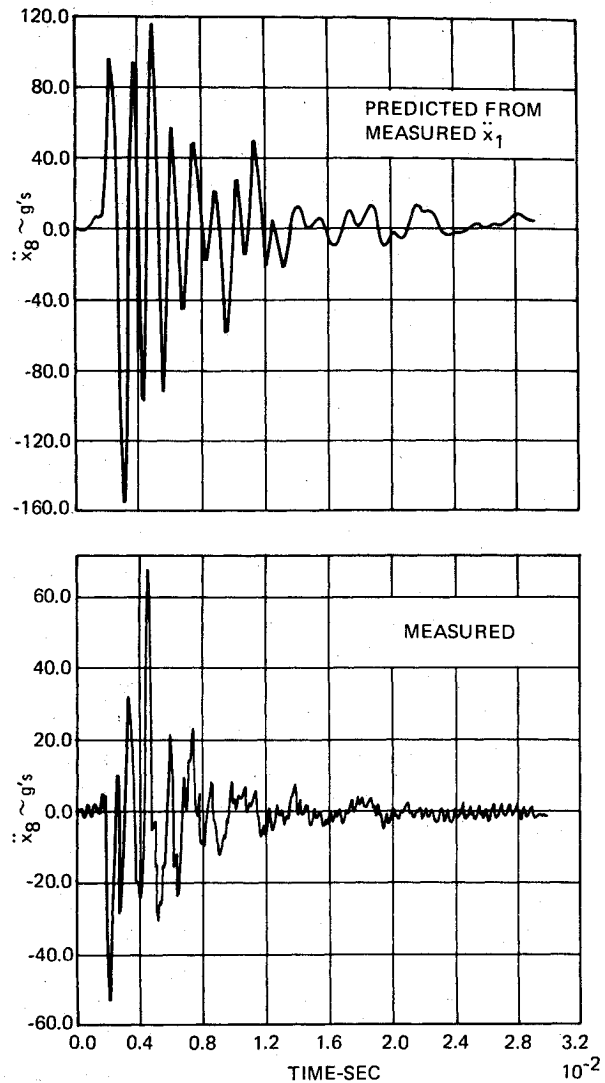


Fig. 4 Time history of \ddot{x}_8 predicted from measured \ddot{x}_I , and measured directly.

corresponding spectrum, together with that of \ddot{x}_8 predicted from the measured \ddot{x}_I , and that of the measured \ddot{x}_8 , are plotted in Fig. 5. It can be concluded, from the close agreement between the two spectra derived from predicted responses, that a synthesized acceleration time history of the form of Eq. (10) provide a good approximation to actual shock response for purposes of evaluating transmitted shock response.

Response from Simulated Shock Event

It was postulated that, at least for the system being analyzed, the variation of x_I could be predicted from a numerical simulation using a model with only a few degrees of freedom, even though to obtain x_8 by direct simulation would

Table 2 Coefficients of synthesized \ddot{x}_I

k	f_k, Hz	$S(f_k), g's$	$C_k, g's$
1	30	40	16.1
2	80	100	38.8
3	300	1200	473
4	800	4200	1630
5	2000	7000	2550
6	5000	12,000	4190
7	10,000	18,000	6010

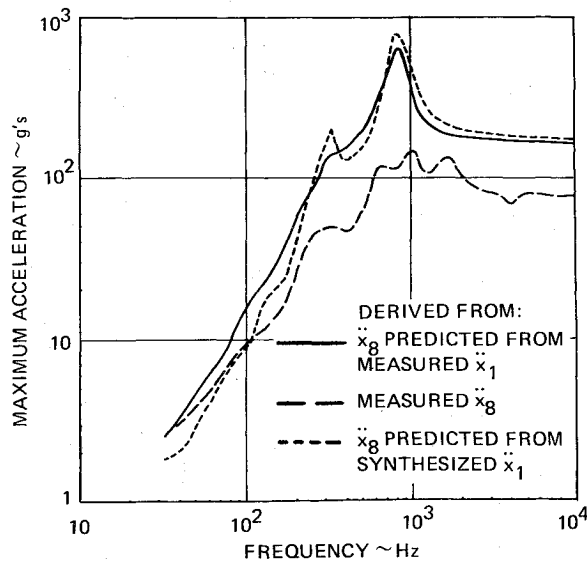


Fig. 5 Shock spectra of \ddot{x}_8 from predicted and measured time histories.

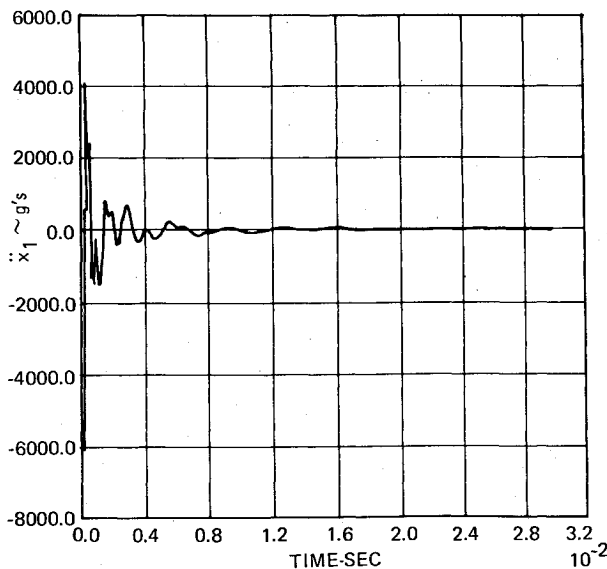


Fig. 6 Time history of \ddot{x}_1 synthesized from shock spectrum.

require the complete model. If so, the response at mass no. 8 can be obtained without the need for a full simulation by employing the result from the simplified model in Eq. (6) and using the parameters of the complete model in constructing g_{81} .

For purposes of simulation, the model was reduced to one having just nine degrees of freedom by simply making the stiffnesses of all springs to the left of mass no. 18 in Fig. 1, including that of the spring connecting 18 with 7, infinite. The shock event was then simulated by numerically integrating the nine coupled equations of motion, using a simple Runge-Kutta formula. The shock was introduced by prescribing initial displacements equal to those that would result by imposing a static preload of the same magnitude as used in the test. While this is in apparent violation of the assumption that all initial displacements are zero, the formulations developed are still applicable, since the condition of the system at the start of integration can be reached by very slowly applying an increasing load to mass no. 1 until the desired preload is achieved and then suddenly removing the load. During the interval while the load is being increase, \ddot{x}_1 would be essentially zero, and the integral in Eq. (6) (with displacement

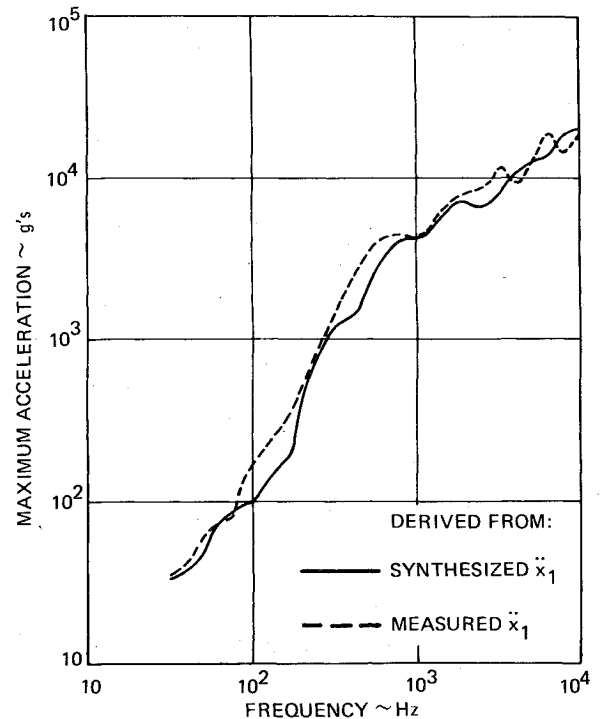


Fig. 7 Shock spectra of \ddot{x}_1 from synthesized and measured time histories.

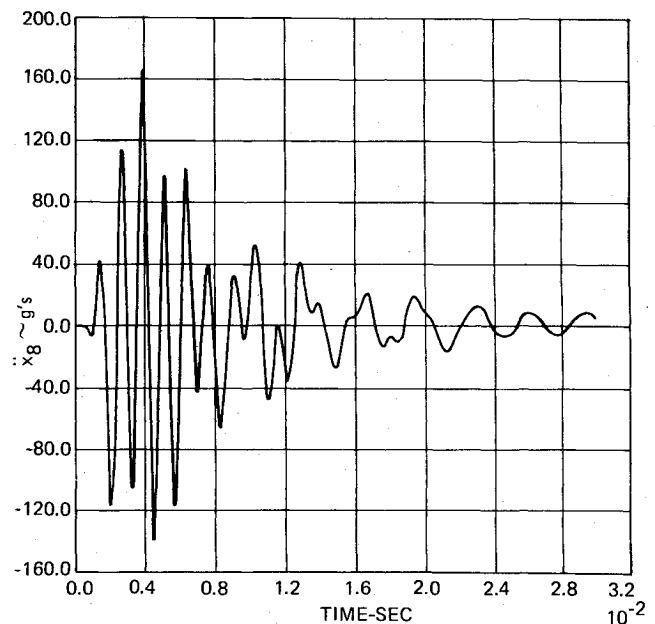


Fig. 8 Time history of \ddot{x}_8 predicted from synthesized \ddot{x}_1 .

replaced by acceleration) would remain zero until the instant the load is removed.

The time history of \ddot{x}_1 obtained from the simulation is shown in Fig. 9. The corresponding shock spectrum is plotted in Fig. 10 together with that of measured response. The simplified model for the system analyzed is seen to provide a very good approximation for predicting \ddot{x}_1 at low frequency, and is adequate for obtaining the high-frequency response. The result of the simulation was used in Eq. (6) to predict \ddot{x}_8 , with g_{81} constructed from the complete 26-degree-of-freedom model. The acceleration time history obtained is shown in Fig. 11 and its shock spectrum, as well as that of the measured response, are plotted in Fig. 12. Agreement between theory and test is seen to be very good. Thus, if shock response in the

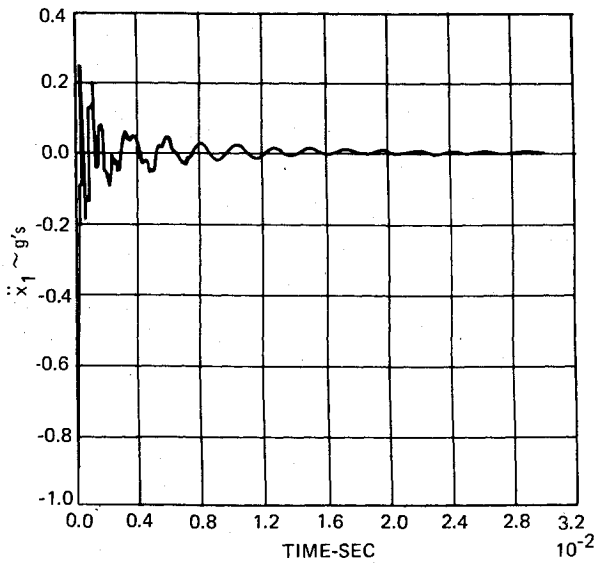


Fig. 9 Time history of \ddot{x}_1 from numerical simulation.

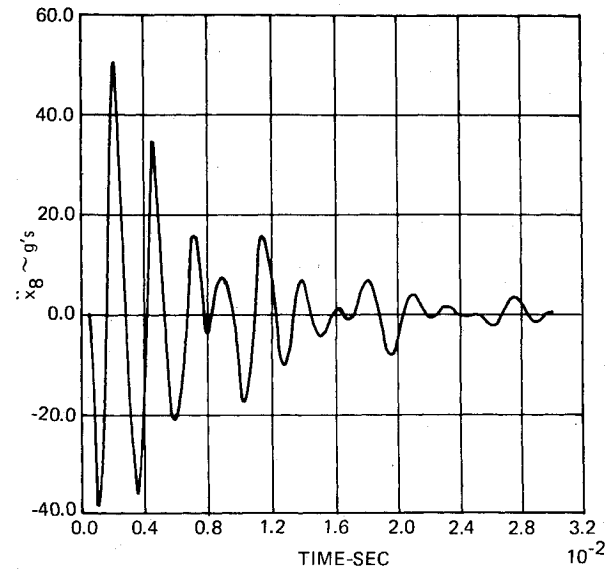


Fig. 11 Time history of \ddot{x}_8 predicted using \ddot{x}_1 from numerical simulation as input to shock transmission analysis.

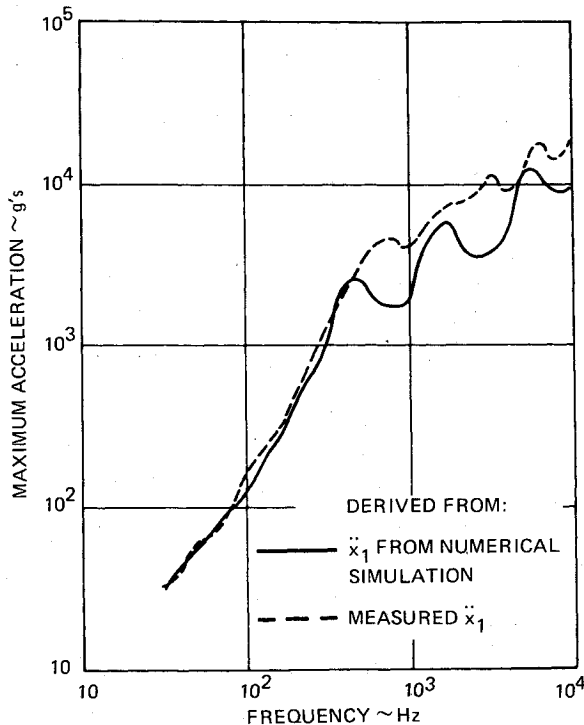


Fig. 10 Shock spectra of \ddot{x}_1 from simulated and measured responses.

vicinity of the load can be adequately simulated with a simplified model, the response at any other point in the structure can be predicted without having to carry out a complete simulation.

IV. Conclusions

The following conclusions can be drawn from the results obtained:

- 1) The formulations developed provide an accurate and practical means for calculating structural response to shock loading at a specified point, given only the response, either measured or predicted, at some other location in the structure.
- 2) Given a shock spectrum of the response at some location, an acceleration time history can be synthesized, as a sum of damped sinusoids, which provides a good approximation to the actual response there for purposes of evaluating transmitted shock response.

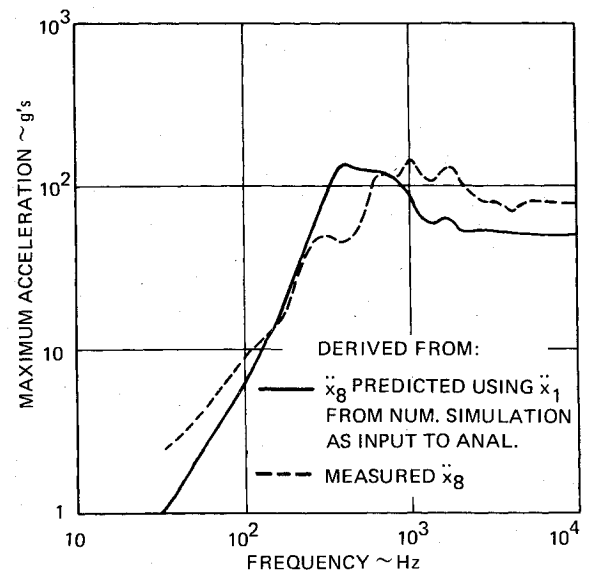


Fig. 12 Shock spectra of \ddot{x}_8 from analysis using numerical simulation as input and from measurement.

3) If shock response in the vicinity of the applied loading can be adequately simulated with a simplified model, the response at any point in the structure can be predicted, using the formulations developed for evaluating transmitted shock response, without the need for a complete simulation of system response.

References

- ¹Huebner, K.H., *The Finite Element Method for Engineers*, Wiley, New York, 1975, p. 238.
- ²Ball, R.E., "Comparison of Two Numerical Methods for the Time-Wise Integration of Transient Structural Response," *AIAA Journal*, Vol. 9, Oct. 1972, pp. 2068-2069.
- ³Morino, L., Leech, J.W., and Witmer, E.A., "Optimal Predictor-Corrector Method for Systems of Second-Order Differential Equations," *AIAA Journal*, Vol. 12, Oct. 1974, pp. 1343-1347.
- ⁴Jacobson, M.J., Yamane, J.R., and Brass, J., "Structural Response to Detonating High-Explosive Projectiles," *Journal of Aircraft*, Vol. 14, Aug. 1977, pp. 816-821.
- ⁵Harris, C.M. and Crede, C.E., (eds.), *Shock and Vibration Handbook*, Vol. 2, McGraw-Hill, New York, 1961, p. 23-13.